Ivermectin and Nodulisporic Acid Receptors in *Drosophila melanogaster* Contain Both γ-Aminobutyric Acid-Gated Rdl and Glutamate-Gated GluClα Chloride Channel Subunits

Steven W. Ludmerer,[‡] Vivien A. Warren,[#] Brande S. Williams,[#] Yingcong Zheng,[‡] David C. Hunt,[‡] Michelle B. Ayer,[§] Michael A. Wallace,[⊥] Ashok G. Chaudhary,[⊥] Marjorie A. Egan,[⊥] Peter T. Meinke,[§] Dennis C. Dean,[⊥] Maria L. Garcia,[#] Doris F. Cully,[‡] and McHardy M. Smith*[,#]

Department of Parasite Biochemistry and Molecular Biology, Department of Drug Metabolism, Department of Basic Medicinal Chemistry, and Department of Ion Channels, Merck Research Laboratories, Rahway, New Jersey 07065

Received November 7, 2001; Revised Manuscript Received March 11, 2002

ABSTRACT: ^{35}S-labeled derivatives of the insecticides nodulisporic acid and ivermectin were synthesized and demonstrated to bind with high affinity to a population of receptors in *Drosophila* head membranes that were previously shown to be associated with a glutamate-gated chloride channel. Nodulisporic acid binding was modeled as binding to a single population of receptors. Ivermectin binding was composed of at least two kinetically distinct receptor populations, only one of which was associated with nodulisporic acid binding. The binding of these two ligands was modulated by glutamate, ivermectin, and antagonists of invertebrate γ-aminobutyric acid (GABA)ergic receptors. Because solubilized nodulisporic acid and ivermectin receptors comigrated as 230-kDa complexes by gel filtration, antisera specific for both the *Drosophila* glutamate-gated chloride channel subunit GluClα (DmGluClα) and the GABA-gated chloride channel subunit Rdl (DmRdl) proteins were generated and used to examine the possible coassembly of these two subunits within a single receptor complex. DmGluClα antibodies immunoprecipitated all of the ivermectin and nodulisporic acid receptors solubilized by detergent from *Drosophila* head membranes. DmRdl antibodies also immunoprecipitated all solubilized nodulisporic receptors, but only ∼70% of the ivermectin receptors. These data suggest that both DmGluClα and DmRdl are components of nodulisporic acid and ivermectin receptors, and that there also exists a distinct class of ivermectin receptors that contains the DmGluClα subunit but not the DmRdl subunit. This co-association of DmGluClα and DmRdl represents the first biochemical and immunological evidence of coassembly of subunits from two different subclasses of ligand-gated ion channel subunits.

The invertebrate γ-aminobutyric acid (GABA)-gated Rdl and glutamate-gated chloride channel (GluCl) gene families are members of the ligand-gated ion channel superfamily that includes nicotinic acetylcholine, $GABA_A$, $GABA_C$, glycine, and ionotropic serotonin receptors (*1*, *2*). Both Rdl and GluCl are targets of action for insecticides and anthelmintics (*3*, *4*), but the subunit composition of native invertebrate receptors that contain these subunits is poorly characterized. Mammalian nicotinic acetylcholine and $GABA_A$ receptors have been extensively studied and shown to be pentameric structures composed of two to four closely related yet distinct subunits (*5*, *6*). Native receptors assembled from subunits of different receptor families, however, have not been described.

The *Drosophila* Rdl gene (DmRdl) was initially identified as the gene that confers resistance to the cyclodiene insecticide dieldrin (*7*). The Rdl protein is a member of the GABA-responsive class of ionotropic receptors, but it is phylogenetically distinct from both mammalian $GABA_A$ and $GABA_C$ receptors (*8*−*10*). However, homomeric DmRdl receptors expressed in heterologous systems have biophysical properties that are dissimilar to those observed with native neuronal *Drosophila* GABA receptors (*11*, *12*), suggesting that DmRdl coassembles with other subunits in native receptors.

The glutamate-gated chloride channel family (GluCl) was first identified by expression cloning of subunits of an avermectin-sensitive *Caenorhabditis elegans* chloride channel (*13*). The avermectins, which include ivermectin (IVM),[1] are a family of macrocyclic lactones widely used in human health, animal health, and crop protection (*14*, *15*). The *Drosophila* GluClα subunit (DmGluClα), cloned by homology to a *C. elegans* GluCl gene, can express homomeric channels in Xenopus oocytes that are gated by glutamate, ivermectin, and nodulisporic acid (NA) (*16*, *17*), the latter being a novel indole diterpene, isolated from cultures of the endophytic fungus *Nodulisporium sp.* (*18*, *19*), that possesses high efficacy at killing fleas when orally administered to dogs

* To whom correspondence should be addressed at Merck Research Laboratories, R80N-31C, P.O. Box 2000, Rahway, NJ 07065. Phone: (732) 594-7013. FAX: (732) 594-3925. E-mail: mchardy_smith@merck.com.

[‡] Department of Parasite Biochemistry and Molecular Biology.

[⊥] Department of Drug Metabolism.

[§] Department of Basic Medicinal Chemistry.

[#] Department of Ion Channels.

[1] Abbreviations: ivermectin, IVM; nodulisporic acid, NA; MsCl, methanesulfonyl chloride; confidence interval, C.I.

10.1021/bi015920o CCC: $22.00
Published on Web 04/23/2002

(*20*, *21*). The pharmacology observed with homomeric expression of the DmGluClα subunit in oocytes differs from that of native locust neuronal GluCl receptors, suggesting that DmGluClα, like DmRdl, may also be part of a multisubunit receptor complex (*22*).

High affinity receptor sites have been identified for [^{3}H]-ivermectin ([^{3}H]IVM) and a tritiated amide derivative of nodulisporic acid ([^{3}H]NAmide, *22*) in *Drosophila* head membranes. Binding of [^{3}H]NAmide to these membranes is modulated by glutamate noncompetitively, suggesting the presence of a GluCl subunit in *Drosophila* NAmide receptors (*22*). Furthermore, NA modulates the binding of IVM to these membranes in a biphasic manner, suggesting the existence of multiple populations of receptors. In addition to DmGluClα, a second component of IVM receptors is likely a GABA subunit because IVM noncompetitively inhibits binding of ethynylbicycloorthobenzoate (EBOB), an insecticide shown to bind insect GABA-gated chloride channels (*23*, *24*).

In the present study, the subunit composition of IVM and NA receptors from *Drosophila* head membranes was investigated with both pharmacological and immunological tools. Using [^{35}S]labeled derivatives of IVM and NAmide as radioligands, we show that the NAmide receptor behaves kinetically as a single population, and that its pharmacological properties are consistent with NAmide receptors being coupled to both glutamate and GABA responsive subunits. Furthermore, antibodies specific for either DmGluClα or DmRdl immunoprecipitate all NAmide receptors solubilized from *Drosophila* head membranes. In contrast, there are at least two kinetically distinct populations of IVM receptors, only one of which is associated with the high-affinity NAmide receptor. Saturating concentrations of DmRdl antibodies immunoprecipitate only 70% of the solubilized IVM receptors, although DmGluClα antibodies immunoprecipitate all of these receptors. These data suggest that DmGluClα and DmRdl are coassembled in a heteromeric complex in both NAmide receptors and a subpopulation of IVM receptors found within *Drosophila* head membranes, and that other IVM receptors in these membranes contain DmGluClα but lack DmRdl. These findings represent the first biochemical documentation that GluCl and Rdl subunits coassemble *in vivo*.

MATERIALS AND METHODS

Generation of DmGluClα, DmRdl, and C. elegans GluClα1 Antisera. Polyclonal rabbit antisera were raised against synthetic peptides whose sequences were selected from the highly diverged M3-M4 intracellular loop of DmGluClα (accession number U58776), DmRdl (accession number M69057), and *C. elegans* GluClα1 (accession number U14524). Peptides (*25*) were synthesized by Research Genetics, Inc. (Birmingham, AL); rabbit antisera were produced by Covance, Inc. (Denver, PA). DmGluClα antisera Gcl3 was generated against the peptide sequence ^{376}KPLVRHPGDPLALEKR^{391}. DmGluClα antisera Gcl5 was generated against the peptide sequence ^{340}NMHKENMKKKRRDLEQASLDAA^{361}. DmRdl antisera Rd7 was generated against the peptide sequence ^{356}KRIQMRKQRFMAIQKIAEQKKQQLD^{380}. *C. elegans* GluClα1 antisera Cea1 was generated against the peptide sequence ^{363}NKQGVERKARTEREKAEIPLLQN^{385}.

Scheme 1: NA and Derivatives of NA and IVM

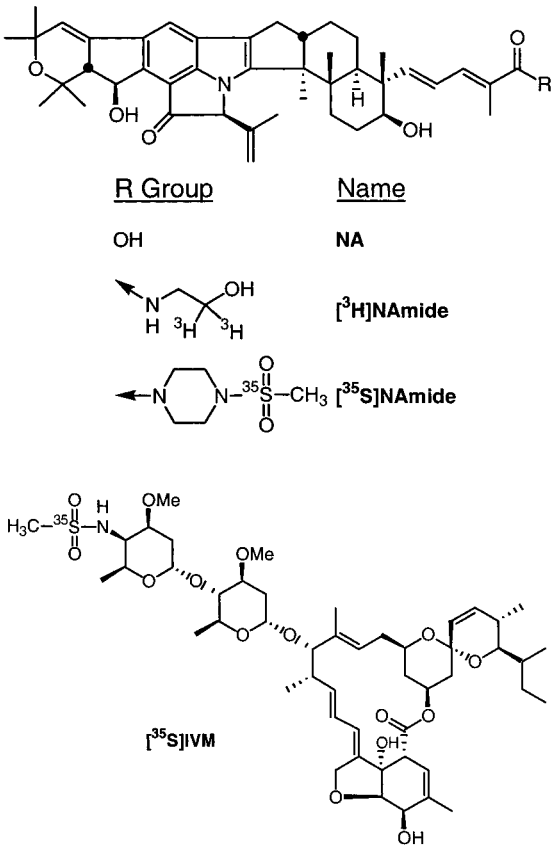

Preparation of [^{35}S]NAmide. A 10-mL tapered conical flask was charged with 22.0 mCi of [^{35}S]methanesulfonyl chloride (MsCl) (*26*) in dichloromethane (3 mL). The solution was concentrated at atmospheric pressure in a 65 °C oil bath to 100 μL. A small crimp-cap vial was charged with the NAmide precursor (8 mg, compound 22 in ref *27*), dichloromethane (50 μL), and a magnetic stir bar. To this vial was added the [^{35}S]MsCl in dichloromethane (100 μL). The tapered flask was washed with dichloromethane (2 × 50 μL), and these washes were added to the reaction mixture. Triethylamine (5 μL) was added to the reaction mixture, and the sample was stirred for 2 h at room temperature. The mixture was diluted with dichloromethane (3 mL), transferred to a 25-mL conical flask, and washed with 0.5% $NaHCO_3$ (3 mL). The aqueous portion was washed with dichloromethane (2 × 2 mL). The combined organic extracts were evaporated to near dryness under a stream of nitrogen gas and diluted with 300 μL of mobile phase (methanol/water, 1:1 v/v). The crude product was purified by using semi-preparative HPLC (Luna phenyl-hexyl, 250 × 10 mm); 85 A:15 B over 30 min; A = methanol; B = water containing 0.1% $HClO_4$; at UV = 240 nm and flow rate 4 mL/min). Combined fractions were neutralized with $NaHCO_3$ solution. Isolation of final product was accomplished using a sep-pac (YMC ODS C18, 300 mg) and yielded [^{35}S]NAmide (Scheme 1, compound 25 in ref *27*) in >99% radiochemical purity as determined by analytical HPLC. The total activity obtained was 9.3 mCi with specific activity 908 Ci/mmol or 1097 mCi/mg as determined by LC/MS. Over the course of eight syntheses, the specific activity ranged from 525 to 1291 Ci/mmol on the reference date.

Preparation of [^{35}S]IVM. A 10-mL tapered conical flask was charged with 24.0 mCi [^{35}S]MsCl (*26*) in dichloromethane (3 mL). The solution was concentrated at atmospheric pressure in a 65 °C oil bath to 100 μL. A small crimp-cap vial was charged with the [^{35}S]IVM precursor (9 mg of 4″-desoxy-4″-epi-amino-IVM, compound 3 in ref *28*), dichloromethane (100 μL), and a magnetic stir bar. To this vial was added [^{35}S]MsCl in dichloromethane (100 μL). The flask was rinsed with dichloromethane (2 × 50 μL), and the rinses were added to the reaction mixture. 4-(Dimethylamino)pyridine (15 mg) was added to the reaction mixture, and it was stirred for 2 h at room temperature. The mixture was diluted with dichloromethane (3 mL), transferred to a 25-mL conical flask, and washed with 0.5% $NaHCO_3$ (3 mL). The aqueous portion was washed with dichloromethane (2 × 2 mL). The combined organic extracts were evaporated to near dryness under a stream of nitrogen gas and diluted with 500 μL of mobile phase (acetonitrile/water, 1:1 v/v). The crude product was purified by using semipreparative HPLC (Zorbax Rx-C8 (250 × 10 mm); 60 A: 40 B over 30 min; A = acetonitrile; B = water containing 0.1% TFA; at UV = 254 nm and flow rate 4 mL/min). Combined fractions were collected. Isolation of final product utilizing a sep-pac (YMC ODS C18, 300 mg) yielded [^{35}S]IVM, 7.3 mCi, (Scheme 1, compound 25 in ref *28*), in >99% radiochemical purity as determined by analytical HPLC. Over the course of 10 syntheses, the specific activity ranged from 600 to 1035 Ci/mmol on the reference date.

To calculate current specific activity of a radiolabeled compound at submaximal specific activity, the following formula was used:

$$SA_{Curr} = F/[1/\{SA_{Ref} - [(1 - F)/SA_{Theo}]\}]$$

where the specific activities are current, at the original reference date and at maximum theoretical specific activity, and F is equal to 0.992^D, where D is the number of days from the reference date to the date when the experiment was subject to scintillation analysis. SA_{Theo} was 1498 Ci/mmol.

Preparation of Drosophila Head Membranes. D. melanogaster (Oregon R) were cultured by standard techniques, and adult flies were harvested and stored frozen at −70 °C. The heads were separated from the bodies by vigorous shaking while flies were frozen, followed by sieving. Heads derived from 5 g of whole flies (approximately 20 mL of loosely packed flies) were homogenized in 20 mL of ice cold 50 mM HEPES pH 7.0 using a Brinkmann Polytron. The homogenate was filtered through two layers of cotton gauze and then centrifuged at 500*g* for 5 min. The supernatant was centrifuged at 20000*g* for 15 min, and the resulting pellet was resuspended at ∼1 mg of protein/mL in 50 mM HEPES pH 7.0, and stored at −70 °C. *C. elegans* membranes were prepared as previously described (*29*).

Binding of [^{35}S]IVM and [^{35}S]NAmide to Drosophila Head Membranes. Binding of [^{35}S]NAmide and [^{35}S]IVM was determined similarly to procedures described previously (*22*). Briefly, 1 μg of membrane protein was incubated with radioactive ligand (3 pM for assays conducted at a fixed concentration of radioligand) at room temperature for a minimum of 1 h in a 3 mL final volume of binding buffer (50 mM HEPES−KOH, pH 7.5, 0.1 mg/mL bacitracin, and 2% dimethyl sulfoxide). Nonspecific binding was determined in the presence of 100 nM unlabeled ivermectin or 100 nM NA. Separation of bound from free ligand was achieved by addition of 3 mL of ice cold wash solution (0.5% Triton X-100) followed by rapid filtration through Whatmann GF/C glass fiber filters that had been soaked in 0.15% Triton X-100, 0.25% polyethyleneimine. Radioactivity retained on filters was determined by liquid scintillation techniques.

Association of the radioligands to their receptor was determined as follows: at zero time, radioligands were added to beakers containing all other components, and then appropriate volumes of this mixture were rapidly pipetted into separate test tubes. The contents were harvested at the times indicated in the figure by the filtration procedure described above. For the data depicted in Figure 3, a different methodology was used. Test tubes with or without aliquots of NA or IVM were prepared to which radioligand was added. To initiate the binding reaction (zero time), a large aliquot of membranes was pipetted into each test tube. This methodology required a minimum of two separate pipettings into the same test tube, which doubled the error due to the pipetting, but also minimized systematic differences in radioligand concentration.

Binding Data Analysis. See appendix.

Solubilization of IVM and NAmide Receptors from Drosophila Head Membranes. Approximately 20 fmol of receptors were incubated with ∼0.1 nM [^{35}S]NAmide or [^{35}S]IVM in 100 μL of binding buffer for 1−2 h at room temperature. Nonspecific binding was determined in the presence of 100 nM unlabeled IVM. At the end of the incubation period, membranes were diluted to 950 μL with solubilization buffer (10 mM HEPES, pH = 7.5, 150 mM NaCl, 0.1 mg/mL bacitracin) at 0 °C, and 50 μL of 10% lysophosphatidylcholine (LPC) was added dropwise, mixed by gentle pipetting, and the solution incubated on ice for 30 min. Material solubilized by 0.5% LPC was clarified by centrifugation at 100000*g* for 45 min in an Optima TL ultracentrifuge (Beckmann Instruments, Palo Alto, CA). *C. elegans* membranes were prepared as previously described and [^{35}S]IVM binding conducted as with *Drosophila* head membranes described above. [^{35}S]IVM binding and solubilization of [^{35}S]-IVM-labeled receptors from *C. elegans* membranes was performed identically to that of *Drosophila* receptors except that (3-[(3-cholamidopropyl)-dimethylammonio]-1-propanesulfonate) was substituted at 1.0% final concentration for LPC.

Size Fractionation of Solubilized IVM and NAmide Receptors from Drosophila Head Membranes. Drosophila head membranes were incubated with either [^{35}S]IVM or [^{35}S]-NAmide, and solubilized as described above. The LPC-solubilized extract was concentrated 5- to 10-fold on a Centricon 30 spin column. A total of 200 μL of solubilized, concentrated membrane extract was loaded onto a Superose 6 FPLC column equilibrated with 10 mM HEPES, 150 mM NaCl, 0.1% LPC at a flow rate of 0.5 mL/min at 4 °C. Fractions of 0.5 mL were collected and analyzed.

Immunoprecipitation of Solubilized IVM and NAmide Receptors. Antisera was mixed with protein A:Sepharose beads overnight at 4 °C at a ratio of 2 mL of antisera/mL of bed volume of protein A:Sepharose (binding capacity 20 mg of IgG/mL of bed volume of resin). The resin was pelleted by low-speed centrifugation, washed a minimum of 5 times with 10 mM HEPES pH 7.5, 150 mM NaCl, 0.1 mg/mL

bacitracin, and resuspended in the same buffer to twice the resin bed volume. One unit of IgG:protein A Sepharose in the immunoprecipitations is defined as one milliliter of the final resuspension of beads.

IgG:protein A Sepharose suspension (0.5 unit) was incubated with 1 mL of solubilized prelabeled receptors for 2 h at 4 °C. For antibody titrations, total protein A:Sepharose was kept constant, and specific antisera coupled beads were mixed with nonpreabsorbed beads in appropriate ratios to keep the bed volume constant. Following incubation, the resin was recovered by low-speed centrifugation, and the supernatant was removed and filtered to determine the amount of receptors not removed by the antibody coated beads. The pellets were washed 5 times with ice-cold Triton wash buffer (0.1% Triton X-100, 50 mM HEPES, pH 7.5, 150 mM NaCl, 0.1 mg/mL bacitracin), resuspended in CytoScint (ICN), and bead-associated radioactivity was determined by liquid scintillation techniques. For sequential immunoprecipitations, the supernatant from the initial immunoprecipitation was incubated with another aliquot of IgG: proteinA Sepharose, and the incubation times were reduced to 90 min.

Immunoprecipitation experiments shown in this work are complete single experiments where the data points are averaged from two or more replicate samples within the experiment. To further verify reproducibility, complete experiments were repeated a minimum of three times employing antisera obtained from at least two different rabbits immunized with the same peptide sequence.

Materials. IVM and NA were from the Merck sample collection. Lysophosphatidylcholine was from Sigma (St. Louis, MO). rec-Protein A Sepharose 4b was obtained from Zymed (S. San Francisco, CA). Lindane isomers were from Chem Service (West Chester, PA).

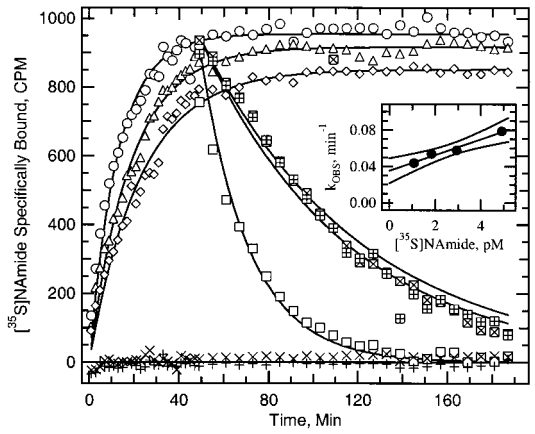

FIGURE 1: Binding of [^{35}S]NAmide to head membranes from *Drosophila melanogaster*. Samples assayed in the presence of IVM (+) or NA (×), both at 0.1 μM, were used to define nonspecific retention of radioactivity by the filter. They averaged 134 ± 6 CPM (mean ± SD, $n = 96$). 134 CPM has been subtracted from all data points depicted. Samples without competing NA or IVM were in a final volume of 1 mL (○), 3.5 mL (△) or 5 mL (◇); for figure clarity, samples run at 2 mL final volume are not depicted. Data were fitted to a monoexponential association model (solid lines). From the exponential association model, k_{OBS} were generated, and the inset shows these values plotted vs the concentration of free [^{35}S]NAmide used. The slope of the line describing these data points is 1.44×10^8 M^{-1} s^{-1}, and the intercept is 0.00059 s^{-1}. The curves in the inset are the 95% confidence bands (Igor Pro). To independently measure the dissociation rate, ligand and membranes were first incubated for 48 min to allow for association, then 0.1 μM NA (boxed x sign), 0.1 μM NA plus 1 mM GABA (boxed plus sign), or 0.1 μM NA plus 1 mM glutamate (□) were added. These samples were distributed and harvested at the times indicated. These data were modeled as a monoexponential decay with a common initial amount bound of 960.9 CPM, using the global fit package in Igor. The fitted exponential decay rates were 0.00026 s^{-1} for both NA and NA plus GABA, and 3-fold higher at 0.00077 s^{-1} for NA plus glutamate.

RESULTS

Drosophila Head Membranes Contain Populations of High Affinity Binding Sites for [^{35}S]NAmide and [^{35}S]IVM. Both [^{3}H]IVM and [^{3}H]NAmide were shown to have dissociation constants below 50 pM (*22*). Therefore [^{35}S]IVM and [^{35}S]-NAmide (Scheme 1) were synthesized, generating radioligands with 25−50-fold higher specific activity, and allowing quantitation of much lower levels of receptor. Binding of the novel ligand [^{35}S]NAmide was inhibited by NA, IVM (Figure 1), and *N*-(2-hydroxyethyl)nodulisporamide (Scheme 1); nonspecific binding was relatively low with [^{35}S]NAmide (134 CPM, Figure 1).

To rigorously identify the binding site, time and concentration dependencies of the association of the radioligand to the binding sites were studied; it was concluded that for the purposes of this study, [^{35}S]NAmide bound to a single high affinity site in these membranes (appendix). The association of [^{35}S]NAmide with membranes in the absence of competitor was both time- and concentration-dependent (Figure 1 and inset). The time course of association of [^{35}S]NAmide was measured at four concentrations, with three of the data sets depicted (Figure 1). These four data sets were fit to a monoexponential association function. Then the k_{OBS} for the monoexponential fits were plotted vs the concentration of [^{35}S]NAmide (see inset Figure 1); the regression line of the data has the slope of k_1 and intercept of k_{-1} (*22*). Over four repetitions of this experiment, the geometric mean value of the association rate constant, k_1, was 1.24×10^8 M^{-1} s^{-1} [Confidence Interval (C.I.) 1.05×10^8 to 1.46×10^8 M^{-1} s^{-1}]. The geometric mean value for the dissociation rate, k_{-1}, was 0.00031 s^{-1} (C.I. 0.00018−0.00055 s^{-1}, $n = 4$). The time course of dissociation of [^{35}S]NAmide was measured directly by first allowing ligand and receptor to associate, and then adding a large excess of NA or IVM and following the dissociation reaction (Figure 1). This resulted in an geometric mean value for the [^{35}S]NAmide dissociation rate k_{-1} of 0.000208 s^{-1} (C.I. 0.000168−0.000258 s^{-1}, $n = 4$), consistent with the indirectly derived k_{-1} but with a smaller error, and corresponding to half-times with a range of 45 to 67 min.

As with [^{3}H]NAmide (*22*), 1 mM glutamate, but not 1 mM GABA, increased the rate of dissociation of [^{35}S]-NAmide by 3.15-fold (C. I. 2.66−3.73-fold, $n = 4$). The dissociation constant K_D can be calculated by dividing k_{-1} by k_1; the value is 2.80 to 1.70 pM, using either the value of k_{-1} derived from k_{OBS} or the directly determined k_{-1}. The K_D derived from direct measurement of the equilibrium binding was 3.42 pM (C.I. 2.36−4.95 pM, $n = 4$), which is similar to the kinetically derived measurements. The B_{max} measured using [^{35}S]NAmide was within 10% of the B_{max} using [^{3}H]NAmide in an experiment performed in parallel; the B_{max} was 1.44 pmol/mg of protein (SD 0.37, $n = 7$). Thus, [^{35}S]NAmide bound with high affinity to the same

single binding site within these membranes as the binding site previously described for [^{3}H]NAmide (*22*).

The binding of [^{35}S]IVM (Scheme 1) to *Drosophila* head membranes was more complex than that of [^{35}S]NAmide. The equilibrium binding measured after 24 h resulted in a B_{max} of 2.55 pmol/mg of protein (SD 0.37, $n = 7$) and the K_D was 3 pM (data not shown). After 48 h equilibration, the equilibrium binding K_D of [^{35}S]IVM could be modeled by binding of ligand to a single site (Figure 2A) with an affinity of 0.229 pM; in the presence of saturating NA, inhibition of [^{35}S]IVM binding to approximately half of the sites was observed with a small shift in the K_D to 0.431 pM; the B_{max} was decreased by 50% relative to the B_{max} seen in 24 h ($n = 4$). The association of [^{35}S]IVM with its receptors was not compatible with binding of the ligand to a single high affinity receptor population, but was consistent with a model where it bound to two (or more) receptor types in these membranes. Therefore, when varying both the concentrations of [^{35}S]-IVM and time of association in the binding assays (Figure 2B), the data better fit a biexponential association process rather than a monoexponential process (see appendix).

The directly measured dissociation rate was 0.000014 s^{-1} (C.I. 0.000009−000023 s^{-1}, $n = 5$), which corresponds to a half-time of greater than 500 min. Data were obtained for 1.5−3.2 h after initiation of dissociation. This time frame represents only a small fraction of the dissociation curve; there could easily exist an undetected population of receptors that dissociate more slowly. Collectively, these results show that [^{35}S]NAmide and [^{35}S]IVM bind differently to *Drosophila* head membranes. Whereas [^{35}S]NAmide binds to a single population, [^{35}S]IVM binds to more than one population of receptors. The difference in the binding populations, combined with the known sensitivity of ≈50% of the IVM sites to NA (Figure 2A), suggested that if the binding of IVM was conducted in the presence of NA, the binding data might be fit to separate monoexponential functions. This proved not to be the case (Figure 3). NA-sensitive IVM binding, although highly variable, did fit a single site model; however, the NA-insensitive IVM binding continued to more closely fit the two-site model (Figure 3). Therefore, these data indicate that there are more than two distinct components of IVM binding to *Drosophila* head membranes.

Previously, it was shown that the [^{3}H]NAmide binding site was associated with a GluCl channel. Figure 4 shows that [^{35}S]NAmide binding was stereoselectively inhibited by the known invertebrate GABAergic antagonists α- and γ-hexachlorohexane. These results suggested that a GABA-responsive subunit is also associated with the [^{35}S]NAmide binding site. Multiple populations of IVM receptors with distinct subunit compositions could account for the two or more distinct IVM binding sites observed. Consequently, the possible coassembly of the glutamate-responsive subunit DmGluClα and the GABA-responsive subunit DmRdl within native IVM and NAmide receptors from *Drosophila* head membranes was investigated.

Solubilization of Drosophila IVM and NAmide Receptors. One approach to characterize receptor subunit composition is to immunoprecipitate radioligand-bound receptors from solubilized membrane extracts using subunit-specific antisera. Thus, *Drosophila* head membranes, preequilibrated with [^{35}S]-IVM or [^{35}S]NAmide, were solubilized with LPC; typically 25 and 13% of the IVM and NAmide receptors were

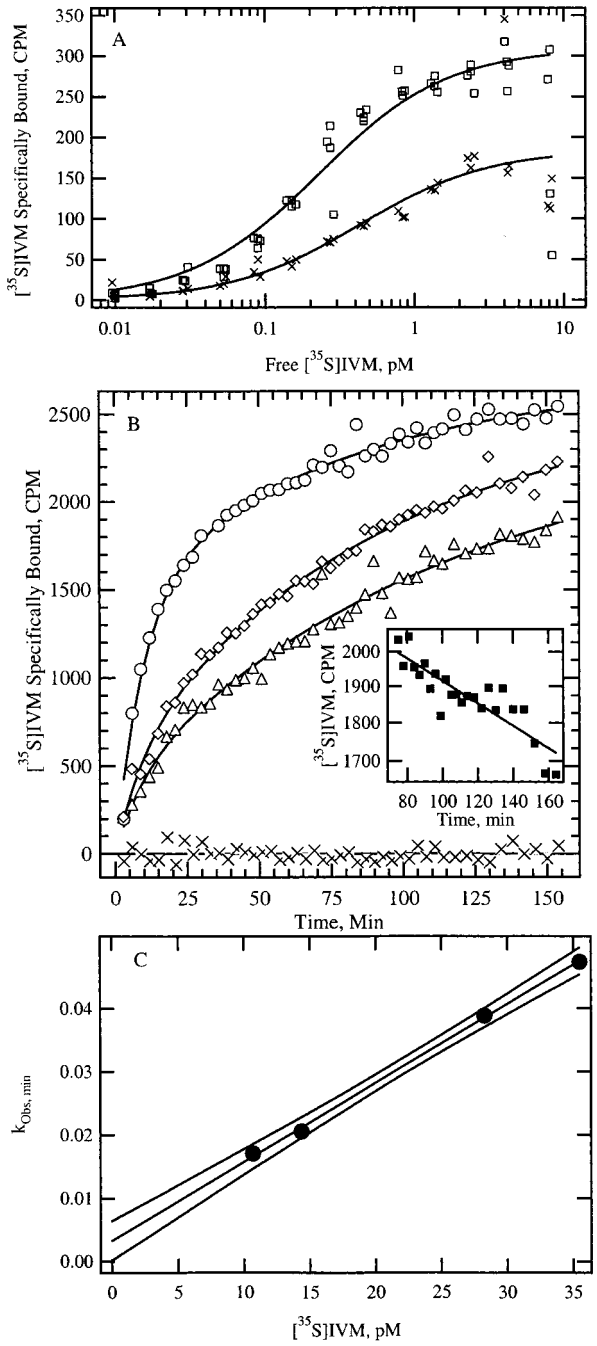

FIGURE 2: Identification of [^{35}S]IVM binding sites in *Drosophila melanogaster* head membranes. (A) Two day equilibrium saturation binding in the absence (□) or presence of 0.1 μM NA (×) showed a specific binding site with a K_D of 0.229 or 0.431 pM, respectively; the B_{max} was decreased in the presence of NA to 60% of that seen in the absence of NA. The B_{max} was decreased by 50% from that seen in a 1 day equilibrium assay ($n = 4$), and to keep total receptor concentration reduced, the assay was run at 0.25 μg of protein per assay point. The values at the highest concentration of ligand are depicted but were not included in the fit. (B) Time course of association of [^{35}S]IVM with *D. melanogaster* head membranes. Membranes and [^{35}S]IVM were combined at zero time in various volumes; samples were aliquoted for individual sampling at the times indicated (volumes were 1 mL [△], 3.5 mL [◊], and 5 mL [○]; the 2-mL samples are not shown for clarity). The solid lines are a biexponential fit to the data (see appendix). The inset shows the directly measured dissociation of [^{35}S]IVM from membranes prebound with [^{35}S]IVM (2 mL volume) on a logarithmic scale. (C) The *mono*-exponential predicted k_1 and k_{-1} derived from the data shown in panel B (see appendix). The confidence intervals predicted (Igor Pro) are indicated by the curved lines.

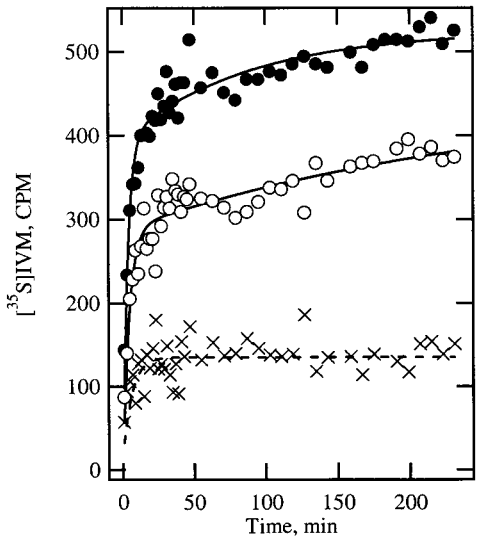

FIGURE 3: Association of [^{35}S]IVM to *Drosophila* head membranes in the presence of NA. Time course of association of [^{35}S]IVM with receptor in the absence (●) or presence (○) of 1 μM NA; the difference between binding in the absence and in the presence of 1 μM NA (×) is also plotted (nonspecific average = 134 ± 12, N = 46, has been subtracted from the data depicted). The data were fitted to a biexponential (solid lines) association model or monoexponential model (dashed line). The data exhibit more variability due to the inherent pipetting error (see Methods). Similar results have been seen in four similar experiments.

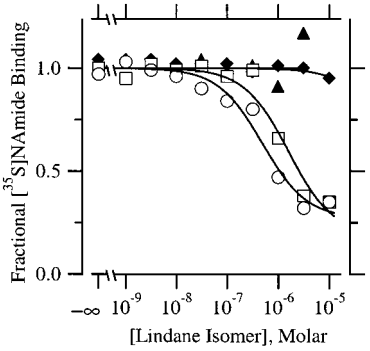

FIGURE 4: The binding of [^{35}S]NAmide is modulated by GABAergic ligands: inhibition of [^{35}S]NAmide binding by isomers of hexachlorohexane. *Drosophila* head membranes were incubated with 3 pM [^{35}S]NAmide for 1 h in the presence of α-HCH (○), β-HCH (▲), γ-HCH (□), or δ-HCH (■). Similar results have been seen in two other experiments.

recovered in a high-speed supernatant after solubilization (S-100). The presence of intact receptor was determined by a filtration assay for [^{35}S]ligand; only conformationally intact receptors retain binding of the noncovalently bound ligand. Yield of intact receptor in detergent solubilized extracts was poor when other detergents were substituted for LPC (data not shown), including detergent conditions successful in solubilizing mammalian $GABA_A$ receptors (*30*, *31*). The interpretation of the experiments on solubilized receptors discussed below is limited to those populations stably solubilized by the LPC solubilization procedure.

To monitor immunoprecipitation of receptor populations using noncovalently bound radioligands, the receptor−ligand complex must have a sufficiently slow dissociation rate such that free radioligand generated during the course of the immunoprecipitation does not obscure interpretation of the experimental results. LPC solubilized S-100 extracts were tested for ligand dissociation at both 22 and 4 °C, the

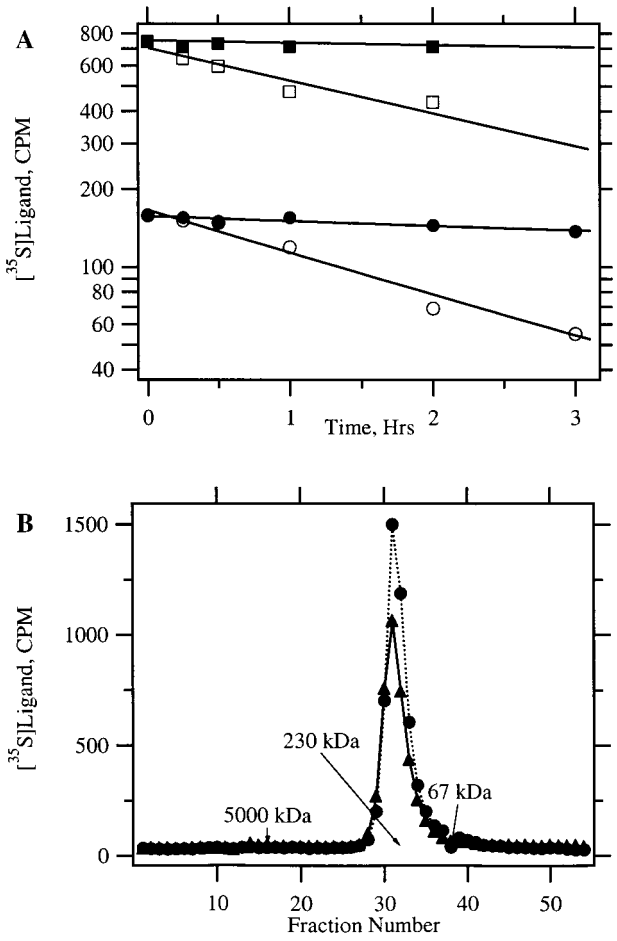

FIGURE 5: Properties of solubilized IVM and NA receptors. (A) S-100 extracts, prelabeled with [^{35}S]NAmide (squares) or [^{35}S]IVM (circles) were incubated at 22° (open symbols) or 4° (filled symbols) for the indicated times and then filtered to assess radioligand-bound receptor. Not shown are data points collected at 20 h. The lines shown are modeling the entire data set (including the 20 h samples) with half-times of dissociation of 20 h or greater for the samples held at 4°, and approximately 2 h for the samples maintained at 22°. The values shown were averaged from triplicate samples; this figure is representative of the two times this experiment was run. (B) 200 μL of [^{35}S]IVM- or [^{35}S]NAmide-labeled, solubilized *Drosophila* head membrane S-100 extracts were size fractionated on an FPLC Superose 6 column. Fractions of 0.5 mL were collected and analyzed for total [^{35}S]IVM (●) or total [^{35}S]NAmide (▲) radioactivity. The values shown are representative of three independent fractionations for IVM receptors and two independent fractionations of NAmide receptors. The column was calibrated by fractionating a cocktail of the following proteins both before and after fractionation of the IVM and NAmide samples, and averaging the values: chymotrypsinogen A, 25 kDa; ovalbumin, 43 kDa; bovine serum albumin, 67 kDa; aldolase, 158 kDa; catalase, 232 kDa; apoferritin, 440 kDa; thyroglobulin; 669 kDa; blue dextran, 5000 kDa. The elution of positions of blue dextran, catalase, and BSA are indicated.

temperatures used in the binding and immunoprecipitation studies, respectively. Solubilized prelabeled receptors had a half-time of dissociation of 2 h when held at 22 °C, consistent with the dissociation from membranes at this same temperature (Figures 1 and 2). When held at 4 °C, receptor−ligand complexes were much more stable; the half-time of ligand dissociation for both [^{35}S]IVM or [^{35}S]NAmide was 24 h (Figure 5A). Thus, in a 2−4 h immunoprecipitation protocol ≥ 89% of the initial bound radioligand remained bound. Further validation of the stability of the receptor−ligand complex was demonstrated in the gel-filtration behavior of

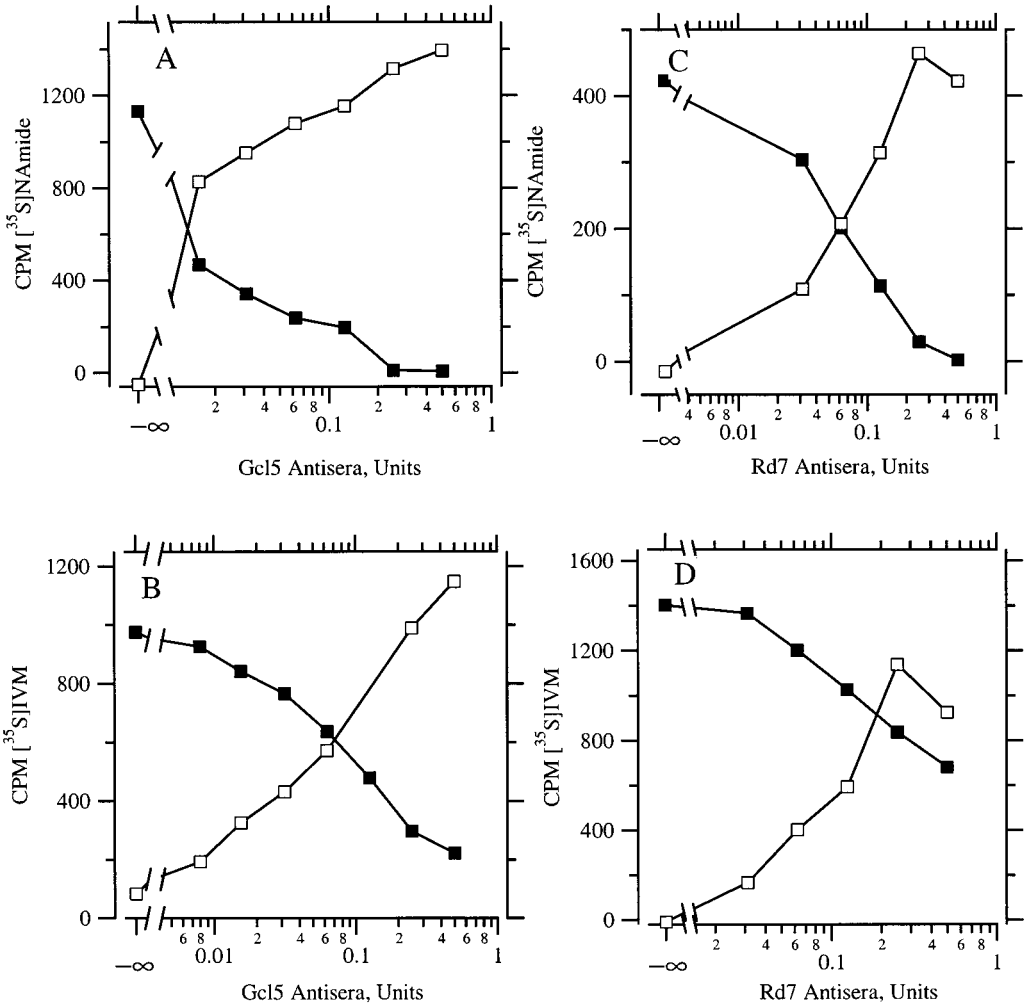

FIGURE 6: Antibody concentration dependence of immunoprecipitation of NAmide and IVM receptors with DmGluCl and DmRdl antisera. *Drosophila* head membranes were incubated with either [^{35}S]NAmide or [^{35}S]IVM, solubilized, and immunoprecipitated with increasing concentrations of either DmGluClα antisera Gcl5 (A and B) or DmRdl antisera Rd7 (C and D), as described in the text. Filter-trapped [^{35}S]NAmide or [^{35}S]IVM within the supernatant are shown as ■; [^{35}S]NAmide or [^{35}S]IVM recovered in the immunoprecipitate pellets are shown as □. The experiments shown in the figure are complete single experiments where the data points are the average of two or more replicate samples. Each experiment was performed in its entirety a minimum of three times, with antisera produced from at least two different rabbits, immunized with the same peptide sequence. Baseline immunoprecipitations using nonimmune antisera (less than 200 CPM) have been subtracted.

the solubilized receptor−ligand complexes. Superose 6 FPLC fractionation of solubilized [^{35}S]IVM and [^{35}S]NAmide receptors yielded superimposable [^{35}S]ligand peaks at a molecular size appropriate for a pentameric ligand-gated ion channel receptor (Figure 5B). The estimated molecular weight of the peak fraction was ~230 kDa, which is the size predicted for a pentameric receptor complex of individual 45−60 kDa subunits. Greater than 93% of the solubilized [^{35}S]ligand loaded onto the column was recovered in the 230-kDa peak fractions. Free [^{35}S]IVM and [^{35}S]-NAmide migrated in the tail column fractions. Therefore, we assume that immunoprecipitation of [^{35}S]ligand using subunit specific antisera was indicative of the presence of the subunit in the ligand complex.

Immunoprecipitation of NA and IVM Receptors with DmGluClα and DmRdl Antisera. Subunit specific antisera were generated to identify DmRdl and DmGluClα subunits within the IVM and the NA receptors (*32*). Antisera specific for either DmGluClα or DmRdl were generated by immunization with synthetic peptides whose sequences were selected from the highly diverged M3−M4 intracellular loop region of DmGluClα or DmRdl. The DmGluClα and DmRdl antisera recognized bacterial fusion proteins with their respective M3−M4 region, but displayed no significant cross-reactivity (data not shown).

Solubilized receptors prelabeled with either [^{35}S]IVM or [^{35}S]NAmide were immunoprecipitated by DmGluClα antisera Gcl5 (Figure 6A, B). Increased concentrations of antisera correlated with both removal of radioligand from the supernatant and recovery of radioligand in the pellet. At sufficiently high antibody concentration, quantitative removal of radioligand from the supernatant occurred, with quantitative recovery of radioligand in the pellet. As a test for antibody specificity, immunoprecipitation was blocked by inclusion of excess DmGluClα peptide, but not by excess DmRdl peptide (data not shown). Similar immunoprecipitation and peptide competition results were observed with a second DmGluClα antisera Gcl3, which was generated against a different peptide sequence within the DmGluClα M3−M4 intracellular loop region (Figure 7A, B and additional data not shown). Thus, 100% of all solubilized IVM and NAmide receptors contain the DmGluClα.

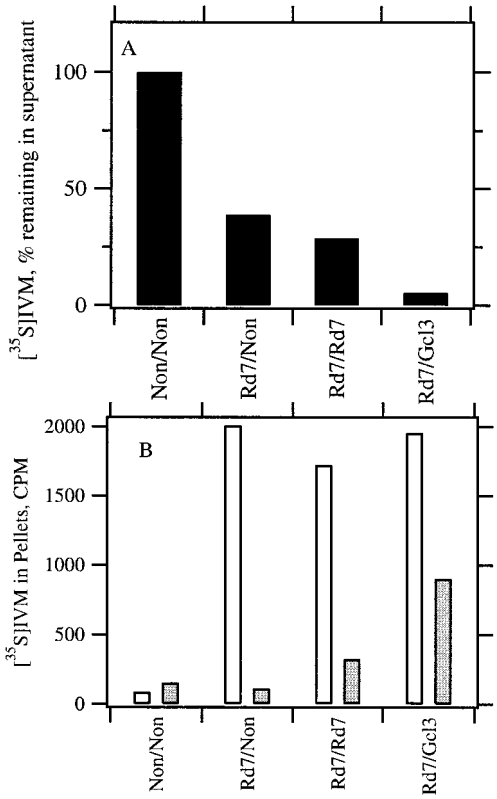

FIGURE 7: Sequential immunoprecipitations with DmRdl antisera Rd7 demonstrate the existence of a pool of IVM receptors that do not contain DmRdl. *Drosophila* head membranes were incubated with [^{35}S]IVM and solubilized as described. 1-mL aliquots of solubilized extract were immunoprecipitated with the indicated antibody. The amount of DmRdl antibody Rd7 was selected to cause > 50% immunoprecipitation of the input IVM receptors. The IgG: protein A Sepharose was recovered by a low-speed spin, and the supernatant was removed and equilibrated with a second aliquot of the indicated antibody. Afterward, the supernatants were analyzed for receptor-bound [^{35}S]IVM remaining after sequential immunoprecipitations, while the pellets from both sets of immunoprecipitations were extensively detergent washed and analyzed for total [^{35}S]IVM. The experiment shown in the figure is a complete single experiment where the data points are the average of two or more replicate samples. The experiment was performed in its entirety a minimum of three times, with antisera produced from at least two different rabbits immunized with the same peptide sequence. (A) Receptor-bound [^{35}S]IVM remaining in the supernatant after sequential immunoprecipitations with either nonimmune antisera or DmRdl antibody Rd7, followed by a second immunoprecipitation with either nonimmune antibody, DmRdl antibody Rd7, or DmGluClα antibody Gcl3. Sequential immunoprecipitations with nonimmune antibody were performed to establish the total IVM receptor population within the supernatant. (B) Immunoprecipitated [^{35}S]IVM recovered after an initial immunoprecipitation with nonimmune antibody or DmRdl antibody Rd7 in the first pellet (open bars) followed by a second immunoprecipitation with either nonimmune antibody, DmRdl antibody Rd7, or DmGluClα antibody Gcl3, in the second pellet (shaded bars).

Solubilized NAmide receptors were also quantitatively immunoprecipitated by DmRdl antisera Rd7 (Figure 6C). As with DmGluClα antibody Gcl5, increasing Rd7 antibody concentrations resulted in quantitative removal of ligand from the supernatant and recovery in the pellet. This demonstrated that DmRdl was also a component of all NAmide receptors within the solubilized extract. In contrast, immunoprecipitation of IVM receptors with Rd7 was incomplete (Figure 6D), and appeared to saturate when ~50% of the solubilized receptors were removed from the supernatant. The level of immunodepletion was not significantly increased when the equivalent of 25 units of DmRdl antibodies, concentrated through peptide affinity purification, was added to a single immunoprecipitation experiment (data not shown). Analogous specificity tests demonstrated that immunoprecipitation of NAmide receptors or IVM receptors was blocked by inclusion of excess DmRdl peptide, but not excess DmGluClα peptide (data not shown).

Table 1: Specificity of DmGluClα and DmRdl Antisera against [^{35}S]IVM Receptors from *Drosophila* vs *C. elegans*

	(fmol of receptor immunoprecipitated)	
	receptors solubilized from	
antisera	*Drosophila*	*C. elegans*
Gcl3	1.9	<0.02[a]
Gcl5	3.1	0.5
Rd7	0.7	<0.02
Ceα1	<0.02	1.9

[a] <0.02 means that the values were below the limit of detection, which was the standard deviation of the replicate nonimmune immunoprecipitations.

To test specificity, the antibodies were assayed for immunoprecipitation of IVM receptors solubilized from *C. elegans* membranes (Table 1). These membranes are populated by multiple subtypes of distinct IVM receptors that contain several different members of the GluCl gene family (*29*, *33*). Approximately 3 fmol (3000 CPM) of either *C. elegans* or *Drosophila* IVM receptors, prelabeled and solubilized, were added to immunoprecipitation reactions, which contained equivalent amounts of *Drosophila* antisera Gcl3, Gcl5, Rd7, or *C. elegans* GluClα antisera Ceα1. Only DmGluClα antisera Gcl5 showed any affinity toward *C. elegans* IVM receptors. An amount of this antibody sufficient to quantitatively immunoprecipitate all of the input *Drosophila* IVM receptors immunoprecipitated ~16% of the *C. elegans* IVM receptors. Subsaturating levels of GluClα and DmRdl antisera Gcl3 and Rd7, which immunoprecipitated approximately 63 and 24%, respectively, of the input *Drosophila* receptors, both showed no cross-reactivity to subunits within *C. elegans* IVM receptors at these concentrations. An amount of a *C. elegans* GluClα1 antibody that immunoprecipitated about two-thirds of the input *C. elegans* IVM receptors was inactive against *Drosophila* IVM receptors. Thus, the DmGluClα and DmRdl antisera were not substantially cross-reactive with IVM receptors from this other invertebrate organism.

An interpretation of the above results (Figure 6) is that DmRdl was a component of some, but not all, of the IVM receptors within solubilized extracts. To test this hypothesis, extracts were immunoprecipitated using DmRdl antisera, and the supernatant was collected and subjected to a second immunoprecipitation using a fresh aliquot of antiserum. When nonimmune antisera was used as a negative control, no [^{35}S]IVM was removed from the supernatant (Figure 7A) or recovered in the pellets (Figure 7B) during either round of immunoprecipitation. Sequential immunoprecipitations with first DmRdl antisera followed by nonimmune antisera cleared the supernatant of 61% of the IVM receptors (Figure 7A). As expected, the receptors were recovered in the first pellet of these immunoprecipitations (using DmRdl antisera); the second immunoprecipitation, using nonimmune antisera, recovered no additional receptors (Figure 7B). When DmRdl

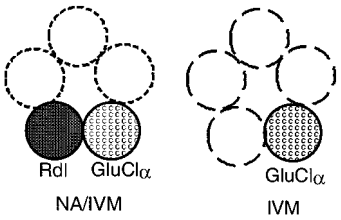

FIGURE 8: IVM receptors from Drosophila head membranes consist of two populations distinguishable in subunit composition. The model illustrates two populations of IVM receptors solubilized from *Drosophila* head membranes that differ with respect to inclusion of DmRdl. One population includes DmRdl and is ~65% of the total population. DmGluClα is a component of both populations. However, only the receptor population in which DmGluClα and DmRdl are coassembled contains high affinity NAmide binding sites. The present work does not address the question of subunit stoichiometry; both DmGluClα and DmRdl are shown as single subunits solely to indicate their presence or absence within these receptors. Additional uncharacterized subunits, shown as empty, may also be components of these receptors. The present model does not postulate whether such subunits are shared or distinct between the two receptor populations, nor does the model postulate about the subunit composition of those receptors not solubilized.

antisera was used in the second immunoprecipitation, only an additional ~8% of the receptors were recovered in the second pellet (Figure 7B); approximately one-third the total receptor population remained in the supernatant. This demonstrated that the lack of quantitative immunoprecipitation of IVM receptors was not due to a limiting concentration of DmRdl antibodies, as sufficient DmRdl antibodies were added to immunoprecipitate any remaining receptors which included DmRdl as a component. A second immunoprecipitation using DmGluClα antisera, however, resulted in quantitative removal of all IVM receptors remaining in the supernatant, with the receptors recovered in the pellet of this immunoprecipitation. Furthermore, the number of receptors recovered in the second immunoprecipitation using DmGluClα antibodies was three times greater than that recovered using DmRdl antibodies. These results, and the results in Figure 3, suggested that there are two populations of IVM receptors, one in which DmGluClα and DmRdl were coassembled, and a second population that contained DmGluClα, without coassembled DmRdl. Comparison of the number of receptors removed and recovered in the sequential DmRdl/DmRdl versus the DmRdl/DmGluClα immunoprecipitations showed that approximately two-thirds of the receptor population within solubilized extracts contained both subunits.

DISCUSSION

This work demonstrates coassembly of DmRdl and DmGluClα in native NAmide and IVM receptors from *Drosophila melanogaster* head membranes. This was accomplished employing two novel insecticide radioligands (Scheme 1) and antisera to DmGluClα and DmRdl. Using a combination of pharmacological and immunological approaches, we established that both DmGluClα and DmRdl are components of native *Drosophila* IVM and NAmide receptors (Figure 8). DmGluClα is a component of all NAmide and IVM receptors in solubilized extracts of *Drosophila* head membranes. DmRdl is also a component of all NAmide receptors and some IVM receptors within these same extracts, but there is a subpopulation of IVM receptors in which DmRdl is absent.

Earlier work demonstrated that IVM receptors consisted of two populations distinguishable by the potency of NAmide inhibition of IVM binding; the B_{max} for high affinity IVM receptors is approximately twice that for high affinity NAmide receptors (*22*). The NAmide binding sites were proposed to be associated with a GluCl receptor because glutamate increased the dissociation rate of NAmide from its binding site by 3-fold, and nodulisporic acid potentiated glutamate activation of *Schistocerca* GluCl channels (*22*). The present binding studies, employing novel [^{35}S]radioligands of higher specific activity, confirmed the earlier observations and further demonstrated that [^{35}S]NAmide binding is conferred by a single receptor population. This receptor population could be modulated by isomers of hexachlorohexane with a stereoselectivity appropriate for their activity as invertebrate GABAergic antagonists (*24*, *34*). These results suggested that a GABA responsive subunit is associated with the NAmide binding previously assumed to be mediated only by a GluCl subunit(s). In addition, these studies demonstrated that the [^{35}S]IVM binding sites are in fact multiple, distinct populations based on the kinetics of binding. This is not surprising given that in *C. elegans* abolition of the IVM binding site is only seen after knocking out three independent GluCl genes (*29*).

The exceptional affinity of these ligands provided a tool for investigating binding at receptor concentrations previously unmeasurable. The K_D for [^{35}S]NAmide (1.7 to 3.6 pM, Figure 1) is ~5 times lower than that of the 12.5 pM value for [^{3}H]NAmide (*22*), while the association rate constants differ by 4.9-fold (1.25×10^8 M^{-1} s^{-1}, Figure 1, vs 2.53×10^7 M^{-1} s^{-1}), accounting for this difference in affinities. The dissociation rates for the two ligands were indistinguishable: 0.000212 s^{-1} (Figure 1) vs of 0.00020 s^{-1} (*22*). The equilibrium affinity of [^{35}S]IVM (0.23 pM, Figure 2) is 10-fold more potent than that reported for *C. elegans* (*29*), and 100-fold more potent than that previously reported for binding of [^{35}S]IVM (*35*) and [^{3}H]IVM (*22*) to the same receptors within *Drosophila* head membranes. The prior measurements may have suffered from an excess of receptor during the measurement; the present results may not be the final equilibrium affinity (appendix). In addition, the immunological experiments would likely have been unachievable without these radioligands of high specific activity and high affinity.

The immunological studies demonstrate direct involvement of the DmRdl and DmGluClα subunits in binding IVM and NAmide. Antisera to either DmGluClα or DmRdl immunodepleted detergent-solubilized *Drosophila* head membrane extracts of NAmide receptors. DmGluClα antisera also immunodepleted solubilized extracts of IVM receptors, but DmRdl antisera immunoprecipitated only ~70% of the IVM receptors within these extracts (Figures 6 and 7). Thus, there exist two populations of IVM receptors that differ with respect to the inclusion of DmRdl. DmGluClα and DmRdl coassembly was also indicated by immunoprecipitation/Western studies which demonstrated that receptors immunoprecipitated by antibodies specific to one of these subunits also contained a protein specifically recognized by antibodies generated against the other subunit (data not shown). The simplest interpretation is that DmGluClα and DmRdl are coassembled within some native IVM and all NAmide receptors solubilized from *Drosophila* head membranes

(Figure 8). We note that the yield of stably solubilized IVM and NAmide receptors are 25 and 13%, respectively; it is possible that the receptor subpopulations solubilized are not representative of the whole.

High affinity NAmide binding exists within that receptor population which contains both DmRdl and DmGluClα. Inclusion of DmRdl into a complex with DmGluClα, however, may not be the sole determinant that confers high affinity NAmide binding. The ~70% of the solubilized IVM receptors which contain DmRdl is higher than the 40% of these receptors that are coupled to high affinity NAmide binding sites in membranes (*22*), suggesting that there are also DmRdl/DmGluClα receptors not coupled to high affinity NAmide binding. In addition, immunoprecipitation with DmRdl antibodies of solubilized IVM receptors that had first been prebound with NA showed a reduction, but not an elimination, in the total IVM receptors immunoprecipitated (data not shown), suggesting the existence of a population of DmGluClα/DmRdl receptors not associated with high affinity NAmide binding. Therefore, it is likely that NAmide receptors contain an additional factor important in conferring native pharmacological properties. We note that better characterized vertebrate ionotropic receptors frequently consist of three or more distinct subunits (*5*, *6*).

That DmGluClα and DmRdl coassemble suggests the existence of receptors responsive to both glutamate and GABA in electrophysiologically experiments. Such receptors have been identified in two other invertebrate systems: *Aplysia* neurons and crayfish muscle (*36*, *37*). However, no indication of Glu/GABA cross-desensitization or subadditivity has been detected in native *Schistocerca* neurons (C. J. Cohen, personal communication), nor have we yet observed electrophysiological data indicative that heteromeric receptors assembled after co-injection of DmGluClα and DmRdl RNA into *Xenopus* oocytes. It is reasonable that an additional subunit (or subunits) is required for DmGluClα and DmRdl to coassemble. In mammalian $GABA_A$ receptors, for example, the β2 subunit is required for the formation of functional α:β and α:β:γ heteromultimers when expressed in CHO cells, and it is possibly required for assembly of native receptors (*38*, *39*). Candidates for a DmGluClα/DmRdl coassembly subunit are not likely to be either LCCH3 or GBR, the other previously characterized *Drosophila* $GABA_A$ homologues (*40*−*42*). Antisera to GBR did not immunoprecipitate IVM receptors, and antisera to LCCH3 immunoprecipitated only ~15% of IVM receptors solubilized from head membranes (interestingly, the same LCCH3 antisera immunoprecipitated more than 75% of an IVM receptor solubilized from membranes prepared from *Drosophila* bodies, data not shown). Further investigations with these antisera against DmGluClα should enable affinity purification of native receptors and identification of additional coassembled subunits.

Pharmacological studies on native insect neuronal preparations demonstrated that insect GABA receptors have a distinct profile that conforms neither to that of mammalian $GABA_A$ nor $GABA_C$ receptors (*11*, *12*, *43*). Some of the biochemical features of invertebrate GABA receptors that distinguish them from mammalian receptors are shared with invertebrate GluCl receptors (*44*). For example, fipronil, the prototype of the phenylpyrazole class of compounds, is a potent insecticide that binds with high affinity to insect but poorly to vertebrate ionotropic GABA receptors (*45*). It blocks the response of oocyte-expressed homomeric receptors of both DmRdl and *C. elegans* GluClβ to GABA and glutamate, respectively (*44*). Furthermore, the Rdl mutation (A302S), demonstrated to confer cyclodiene resistance in *Drosophila*, not only reverses fipronil activity on oocyte-expressed A302S DmRdl homomeric receptors, but the equivalent mutation substituted into *C. elegans* GluClβ results in the same altered fipronil response in oocyte-expressed homomeric GluClβ receptors. Such studies suggest that invertebrate GABA and GluCl subunits share structural features that confer similar pharmacological responses, despite the fact that they may bind different activators.

In *Drosophila*, DmRdl is widely distributed throughout the central nervous system and is a critical mediator of GABAergic responses (*8*, *46*, *47*). It also is the principle target for cyclodienes (*3*). We show that DmRdl is coassembled with DmGluClα in the receptors for two drugs with potential insecticidal activity. This suggests that DmGluClα/DmRdl receptors may be an especially important drug target. A clear understanding of how these two proteins coassemble will further the development of screens for novel compounds with insecticidal activity.

ACKNOWLEDGMENT

The authors would like to thank Dr. Gregory Kaczorowski for his encouragement, numerous thoughtful discussions, and critical reading of the manuscript. We would also like to thank Ann Smith for her critical reading and comments on the manuscript.

APPENDIX: STATISTICAL DECISION-MAKING IN DISCRIMINATING BETWEEN MODELS APPROPRIATE FOR BINDING DATA

McHardy M. Smith

Tritiated ligands are useful for studying ligand receptor interactions when the K_D is in the low nanomolar range, but radioligands of higher specific activity confer greater sensitivity for the measurement of K_D values in the low picomolar range. Measuring K_D values below 100 pM with tritiated ligands while maintaining receptor concentrations below K_D (a crucial requirement for such measurements) often requires both large volumes and long scintillation data acquisition times to achieve an acceptable signal-to-noise ratio. The use of ^{35}S or ^{125}I ligands, possessing typically 40−70 times the specific activity of a tritiated compound, minimizes volumes, receptor concentration, and radioligand consumption without compromising the signal.

With ligands of higher specific activity, one may reexamine membrane receptors that had previously been documented with tritiated ligands to contain a single population of receptors. The membranes may actually contain multiple subpopulations of receptors, distinguishable by their association and dissociation behavior. This is demonstrated in the present work. The statistical means to discriminate between different models of association behavior is the subject of this appendix.

METHODS

In addition to the data analysis methods previously described (*22*), further methods were employed. The kinetics of association of [^{35}S]IVM was modeled with a single site

model, as before. The results from the one site fit were used to calculate the Test of Runs (Prizm 3.0, *48*). If that test showed significance, then a two site model was also fit to the data:

$$B = B_{Eq} - (B_{Eq}Fe^{(-k_{Fast}t)}) - (B_{Eq}[1 - F]e^{(-k_{Slow}t)})$$

where B and B_{Eq} are, respectively, the amount bound at time t and the asymptotic equilibrium amount bound, k_{Fast} and k_{Slow} are the two rate constants of association, and F is the fraction of sites binding with a rate constant of k_{Fast}. For the data in Figure 2A, weights in the fitting were iteratively calculated using the formula

$$\text{weight} = \left[\frac{(y_i - y_p)}{y_i}\right]^2$$

where y_i and y_p equal the actual and predicted data at the ith data point. This weighting scheme weights percentage differences between actual and predicted data points equally across data that spans multiple orders of magnitude; the Igor nonlinear fitting routine was rerun until model parameter values changed less than 2%. The partial F-test was then used to distinguish the better fitting of nested models (*49*, *50*). If the partial F test is significant, another Test of Runs is run on the residuals to determine if a yet more complicated model is still needed. This sequence of tests requires three sequential statistical tests to conclude that a two site is the appropriate model for the data; to ensure that the alpha level of type I errors is not inappropriately high for the three sequential tests, each individual test alpha level was set to $p = 0.0167$.

Association and dissociation rate constants (k_1 and k_{-1}), as well as K_D values from similar multiple experiments, are rates and proportions. As such, they cannot have values less than zero, and cannot arise from a Gaussian distribution. The metrics to report central tendency and population dispersion were the geometric mean and confidence intervals constructed from one standard deviation (67% of the population, C.I.) of the geometric mean, converted back to the arithmetic scale.

RESULTS AND DISCUSSION

In radioligand−receptor association data, there is ample theoretical and experimental precedence for fitting ligand binding to a single receptor population by a monoexponential association model. Data generally are fit to the simplest model possible. However, this is not always an adequate model for the data. In assessing goodness of fit of the simple model, the following statistical tests should be considered. The most simple test is to pose the question: do the data points randomly deviate from the model, or are there systematic deviations of the data points which are not explained by the model. Quantitating the deviation is first done using a less robust test with minimal assumptions, the Test of Runs. In this test, the residuals, which are the differences between the data and the predicted values, are plotted. If the model is a good predictor, the data points will randomly deviate around the zero line of the predicted values. If, however, the data has significant trends where it is not well fit by the model, the residuals will be clustered first on one side of the zero line, and then on the other. These clusters with no zero crossings are termed runs. The expected number of zero-crossings may be calculated from the number of data points. If the model is a poor predictor of the data, then the number of zero-crossings is significantly less than would be predicted by random chance. Consequently, a more complicated model is required to adequately fit the data.

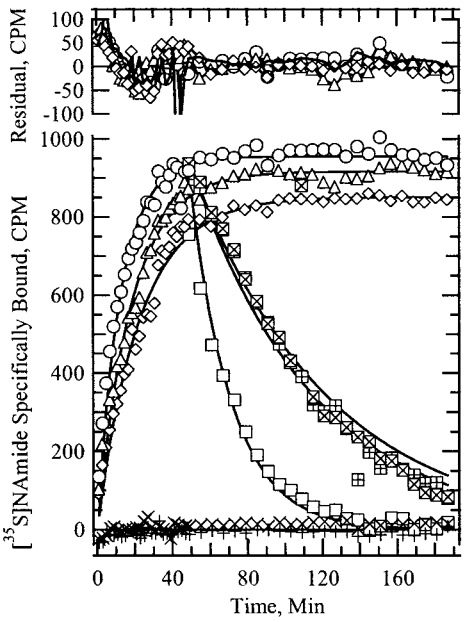

FIGURE 9: Binding of [^{35}S]NAmide to head membranes from *Drosophila melanogaster*. The lower portion of the figure is duplicated from the main text. Symbols are as described in the legend to Figure 1 within the main text. To detect systematic deviation of the data from the model, the difference between the model and the data were plotted in the axis labeled "Residual" using the same symbols; the residual for the 2 mL assay is shown as the solid line without symbols.

The four data sets depicted in Figure 9 were fit to a monoexponential association function. Plotted above these data in Figure 9A are the residuals, which is the difference between the data and the predicted value. A Test of Runs on the residuals indicated a nonrandom deviation of the data from the monoexponential model, which implies that the monoexponential fit may not be an adequate model for the data. This was primarily due to the manner of data collection, where data points were collected initially at three times the terminal data collection rate.

The data were then fit to both the simpler model and the more complicated model. The residual error of the more complicated model has to be decreased by more than a factor necessary to account for the extra fitting parameters to achieve significance, and this test is called a partial F-Test (*49*, *50*). A partial F-test on the data fit to a biexponential model did not show a significantly better fit than the monoexponential model, without weighting the data. Even with weighting of the four data sets during modeling, the error associated with the modeled fast k_{OBS} for the one milliliter reaction was large ($k_{OBS} = 0.62397 \pm 0.2714$ min^{-1}); while this may indicate a different receptor isoform for a small fraction of the binding sites (17 ± 7%, k_{FAST} = 10 times faster than the k_{SLOW} for the bulk of the population), the [^{35}S]NAmide receptor(s) was treated as a single population for the purposes of this study.

The binding of [^{35}S]IVM was more complex. When the samples were incubated for 24 h at a receptor concentration

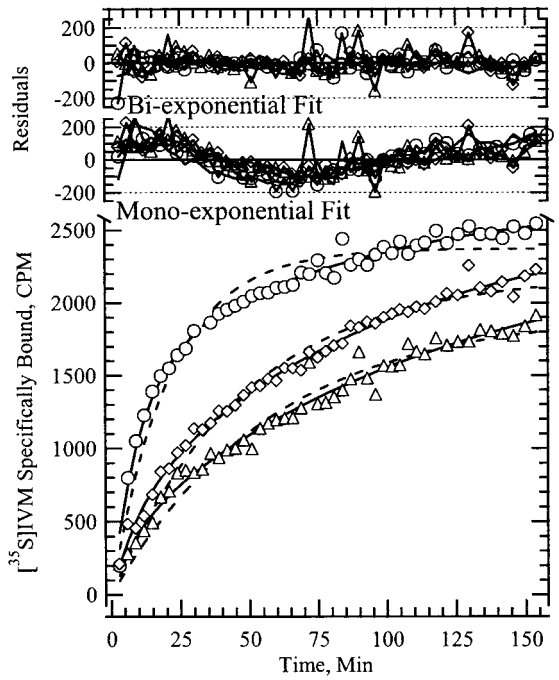

FIGURE 10: The lower portion is the data depicted in Figure 2B, main text. The data were fit to a monoexponential association model (dashed lines). The one-site residuals were calculated and are shown above, using the same symbols as in the lower panel. The results of a Test of Runs using all four data sets was significant in all four cases. Therefore the four data sets were modeled using a two site exponential association model. The residuals calculated from the two site fit are depicted as the uppermost traces. The two fits were compared using a partial F-test and the two site model significant better fit the data in all four cases ($p < 0.008$ to < 0.0004). When subjected to a Test of runs the residuals from the two site fit did not significantly deviate from the model. Therefore, no further modeling was carried out on these data sets.

of ca. 0.2 pM, the K_D measured from the results was 3 pM (range 2−5 pM, $n > 10$). In a 48 h incubation performed in a 12-mL volume (12 fM receptor) over the range of concentrations examined, the equilibrium binding of [^{35}S]-IVM could be modeled by binding of ligand to a single site with the Hill coefficient fixed at 1 (Figure 2A). The presence of saturating NA inhibited [^{35}S]IVM binding to about half of the sites. Without competing NA, the data was better fit to a model of a single binding site where the Hill coefficient was allowed to float; modeled results converged on a solution with a K_D of 0.19 pM and a Hill coefficient of 1.4. An artifact that can produce data that are modeled better with a Hill coefficient greater than one is a situation in which the receptor/ligand solution is not at equilibrium. There were indications that proteolysis and receptor degradation were affecting the results when samples were held for such long incubation periods, accounting for possible nonequilibrium conditions. Therefore, it was not technically feasible to repeat the experiment with substantially longer incubation times and larger incubation volumes. Thus, this estimate of receptor affinity to a single site of 0.23 pM may be an overestimate; there could exist a subpopulation(s) with a higher affinity and not capable of being measured within this experimental design, as it may have been in preequilibrium.

Varying both the concentrations of [^{35}S]IVM and time of association in the binding assays, however, produced data better fit by a biexponential association process (Figure 10, solid lines) rather than a monoexponential process (Figure 10, dashed lines) when compared using a partial F-test. Plots of the residuals for the two models show the quantification of this systematic deviation (upper axes, Figure 10). The data shows large runs of systematic deviations from the model with a one site fit ($p < 0.001$ to < 0.003); however, the residuals were more randomly distributed around the zero line with a two site fit according to a runs test ($p > 0.0167$). This is reflected in the tendency for the data points to adhere more closely to the two site model with only random deviations, as opposed to the systematic deviations from the one site model (Figure 10, dashed lines). The observation that the binding of [^{35}S]IVM to its receptors in *Drosophila* head membranes could be better fit by a biexponential association model was repeatedly found over 15 months, five different syntheses of [^{35}S]IVM, and multiple preparations of membranes.

Plotting the k_{OBS} derived from the *single* site modeling of the data vs [^{35}S]IVM, (allowing for the single site model k_{OBS} to be contaminated with effects from the obvious multisite data) and extrapolating the slope back to the y intercept produces a k_{-1} close to zero (Figure 10). Averaging the k_{-1} from five experiments resulted in a standard deviation larger than the k_{-1} itself. Thus, the actual value was indistinguishable from zero. Although the two k_{OBS} values from the two site models could be used in this analysis, the error in the estimates precluded further analysis of the results.

REFERENCES

1. Vassilatis, D. K., Elliston, K. O., Paress, P. S., Hamelin, M., Arena, J. P., Schaeffer, J. M., Van der Ploeg, L. H., and Cully, D. F. (1997) *J. Mol. Evol. 44*, 501−8.
2. Xue, H. (1998) *J. Mol. Evol. 47*, 323−33.
3. ffrench-Constant, R. H. (1994) *Insect Biochem. Mol. Biol. 24*, 335−45.
4. Eldefrawi, A. T., and Eldefrawi, M. E. (1987) *FASEB J. 1*, 262−71.
5. MacDonald, R. L., and Olsen, R. W. (1994) *Annu. Rev. Neurosci. 17*, 569−602.
6. Betz, H. (1990) *Neuron 5*, 383−92.
7. ffrench-Constant, R. H., Rocheleau, T. A., Steichen, J. C., and Chalmers, A. E. (1993) *Nature 363*, 449−51.
8. Hosie, A. M., Aronstein, K., Sattelle, D. B., and ffrench-Constant, R. H. (1997) *Trends Neurosci. 20*, 578−83.
9. Hosie, A. M., and Sattelle, D. B. (1996) *Br. J. Pharmacol. 119*, 1577−85.
10. ffrench-Constant, R. H., Anthony, N., Aronstein, K., Rocheleau, T., and Stilwell, G. (2000) *Annu. Rev. Entomol. 48*, 449−66.
11. Zhang, H.-G., ffrench-Constant, R. H., and Jackson, M. B. (1994) *J. Physiol. 479.1*, 65−75.
12. Zhang, H.-G., Lee, H.-J., Rocheleau, T., ffrench-Constant, R. H., and Jackson, M. B. (1995) *Mol. Pharmacol. 48*, 835−40.
13. Cully, D. F., Vassilatis, D. K., Liu, K. K., Paress, P. S., Van der Ploeg, L. H., Schaeffer, J. M., and Arena, J. P. (1994) *Nature 371*, 707−11.
14. Campbell, W. (1989) *Ivermectin and Abamectin*, Springer-Verlag, New York.
15. Cleland, T. A. (1996) *Molec. Neurobiol. 13*, 97−136.
16. Cully, D. F., Arena, J. P., Paress, P. S., and Liu, K. K. (1997) U.S. Patent 5,693,492.
17. Cully, D. F., Paress, P. S., Liu, K. K., Schaeffer, J. M., and Arena, J. P. (1996) *J. Biol. Chem. 271*, 20187−91.
18. Ondeyka, J. G., Helms, G. L., Hensens, O. D., Goetz, M. A., Zink, D. L., Tsipouras, O. D., Shoop, W. L., Slayton, L., Dombrowski, A. W., Polishook, J. D., et al. (1995) *J. Am. Chem. Soc. 119*, 8809−16.

19. Ostlind, D. A., Felcetto, T., Misura, A., Ondeyka, J., Smith, S., Goetz, M., Shoop, W., and Mickle, W. (1997) *Med. Vet. Entomol. 11*, 407−8.
20. Shoop, W. L., Gregory, L. M., Zakson-Aiken, M., Michael, B. F., Haines, H. W., Ondeyka, J. G., Meinke, P. T., and Schmatz, D. M. (2001) *J. Parasitol. 87*, 419−23.
21. Shoop, W. L., Zakson-Aiken, M., Gregory, L. M., Michael, B. F., Pivnichny, J., Meinke, P. T., Fisher, M. H., Wyvratt, M. J., Pikounis, B., and Schmatz, D. M. (2001) *J. Parasitol. 87*, 1150−4.
22. Smith, M. M., Warren, V. A., Thomas, B. S., Brochu, R. M., Ertel, E. A., Rohrer, S., Schaeffer, J., Schmatz, D., Petuch, B. R., Tang, Y. S., Meinke, P. T., Kaczorowski, G. J., and Cohen, C. J. (2000) *Biochemistry 39*, 5543−54.
23. Cole, L. M., Roush, R. T., and Casida, J. E. (1995) *Life Sci. 56*, 757−65.
24. Calder, J. A., Wyatt, J. A., Frenkel, D. A., and Casida, J. E. (1993) *J. Comput.-Aided Mol. Des. 7*, 45−60.
25. Tam, J. P. (1988) *Proc. Natl. Acad. Sci. U.S.A. 85*, 5409−13.
26. Dean, D. C., Nargund, R. P., Melillo, D. G., Pong, S. S., Patchett, A. A., Smith, R. G., Chaung, L. P., Ellsworth, R. L., Griffin, P., and Van der Ploeg, L. (1996) *J. Med. Chem. 39*, 1767−70.
27. Meinke, P. T., Ayer, M. B., Colletti, S. L., Li, C., Lim, J., Ok, D., Salva, S., Schmatz, D. M., Shih, T. L., Shoop, W. L., Warmke, L. M., Wyvratt, M. J., Zakson-Aiken, M., and Fisher, M. H. (2000) *Bioorg. Med. Chem. Lett. 10*, 2371−4.
28. Mrozik, H., Eskola, P., Arison, B. H., Linn, B. O., Lusi, A., Matzuk, A., Shih, T. L., Tischler, M., Waksmunski, F. S., Wyvratt, M. J., Blizzard, T. A., Margiatto, G. M., Fisher, M. H., Shoop, W. L., and Egerton, J. R. (1995) *Bioorg. Med. Chem. Lett. 5*, 2435−40.
29. Dent, J. A., Smith, M. M., Vassilatis, D. K., and Avery, L. (2000) *Proc. Natl. Acad. Sci. U.S.A. 97*, 2674−9.
30. Sigel, E., and Barnard, E. A. (1984) *J. Biol. Chem. 259*, 7219−23.
31. Bristow, D. R., and Martin, I. L. (1987) *J. Neurochem. 49*, 1386−93.
32. McKernan, R., Quirk, K., Prince, R., Cox, P. A., Gillard, N. P., Ragan, C. I., and Whiting, P. (1991) *Neuron 7*, 667−76.
33. Cully, D. F., Wilkinson, H., Vassilatis, D. K., Etter, A. and Arena, J. P. (1996) *Parasitology 113*, S191−S200.
34. Olsen, R. W., Szamraj, O., and Miller, T. (1989) *J. Neurochem. 52*, 1311−8.
35. Kane, N. S., Hirschberg, B., Qian, S., Hunt, D., Thomas, B., Brochu, R., Ludmerer, S. W., Zheng, Y., Smith, M., Arena, J. P., et al. (2000) *Proc. Natl. Acad. Sci. U.S.A. 97*, 13949−54.
36. Franke, C. H., and Dudel, J. (1986) *J. Compar. Physiol. A 159*, 591−609.
37. Oyama, Y., Ikemoto, Y., Kits, K. S., and Akaike, N. (1990) *Eur. J. Pharmacol. 185*, 43−52.
38. Connor, J. X., Boileau, A. J., and Czajkowski, C. (1998) *J. Biol. Chem. 273*, 28906−11.
39. Farrar, S. J., Whiting, P. J., Bonnert, T. P., and McKernan, R. M. (1999) *J. Biol. Chem. 274*, 10100−4.
40. Harvey, R. J., Schmitt, B., Hermans-Borgmeyer, I., Gundelfinger, E. D., Betz, H., and Darlison, M. G. (1994) *J. Neurochem. 62*, 2480−3.
41. Henderson, J. E., Soderlund, D. M., and Knipple D. C. (1993) *Biochem. Biophys. Res. Commun. 2*, 474−82.
42. Henderson, J. E., Knipple, D. C., and Soderlund D. M. (1994) *Insect. Biochem. Mol. Biol. 24*, 363−71.
43. Aydar, E., and Beadle, D. J. (1999) *J. Insect Physiol. 45*, 213−9.
44. Smith, M. M., Thomas, B. S., Warren, V. A., Brochu, R., Dick, I., Hirschberg, B., Arena, J., Ludmerer, S. W., Zheng, Y., Cully, D., and Cohen, C. J. (1999) *Soc. Neurosci. Abstracts 25*, 1483.
45. Gant, D. B., Chalmers, A. E., Wolff, M. A., Hoffman, H. B., and Bushey, D. F. (1998) *Rev. Toxicol. 2*, 147−56.
46. Aronstein, K., Auld, V., and ffrench-Constant, R. H. (1996) *Invertebr. Neurosci. 2*, 115−20.
47. Harrison, J. B., Chen, H. H. Sattelle, E., Barker, P. J., Huskisson, N. S., Rauh, J. J., Bai, D., and Sattelle, D. B. (1996) *Cell Tissue Res. 284*, 269−78.
48. Motulsky, H. J. (1999) *Analyzing Data with GraphPad Prism*, GraphPad Software Inc., San Diego, CA.
49. Horn, R. (1987) *Biophys. J. 51*, 255−63.
50. Rodbard, D. (1974) *Clin. Chem. 20*, 1255−70.

BI015920O